Probabilistic Occupancy Filter for Parking Slot Marker Detection in an Autonomous Parking System Using AVM

Minchul Lee, *Student Member, IEEE*, Seokwon Kim, *Student Member, IEEE*, Wonteak Lim, *Student Member, IEEE*, and Myoungho Sunwoo, *Member, IEEE*

***Abstract*— Many car makers have examined parking assistance systems and auto parking systems that automatically find free parking spaces and can park a car. The around view monitoring (AVM) can compensate for the disadvantages of distance-sensor-based detection because it can recognize parking spaces based on parking slot markers instead of empty spaces. However, in the case of AVM-based parking marker recognition, false-positive (FP) features can be detected from 3-D objects and shadows, and the parking slot marker is occluded by the vehicle on which the AVM camera is attached. In this paper, we propose a probabilistic occupancy filter to detect parking slot markers. This filter uses a series of AVM images and onboard sensors to improve the occlusion problem and reduce the FPs from other objects. Each pixel of an AVM image has an occupancy probability of parking slot marker features. The occupancy probability compensates for using vehicle motion and updates using the error model of the AVM system and the performance indicator of the feature extractor.**

***Index Terms*— Occupancy probability, road surface marker, auto parking, around view monitoring (AVM), Bayesian filter.**

I. Introduction

PARKING slot recognition for parking assistance systems and autonomous parking systems uses distance sensors and image sensors. A distance sensor-based parking assistance system recognizes an empty space using ultrasonic sensors and lidar sensors [1]–[3]. Even if an empty space is not a parking space, the system recognizes a parking space when a space that is equal to the width of the vehicle is detected. Distance-sensor-based parking slot recognition is applied in a parking assistance system where a person finally determines a parking space. However, it is difficult to apply in a fully autonomous parking system, where the system judges a parking space and moves the car. The disadvantages of distance based sensors can be compensated for by image sensors such as the Around View Monitoring (AVM) because the image-sensor-based parking space recognition detects spaces based on parking slot markers [4]–[6]. However, the image-based feature extraction sometimes detects false positives because of other objects such as shadows, vehicles, and guidance cones. These false-positive features result in misrecognition of a parking space because of the characteristics of AVM.

Manuscript received July 17, 2017; revised January 19, 2018, May 14, 2018, and June 26, 2018; accepted July 9, 2018. This work was supported in part by the BK21 Plus Program through the Ministry of Education, South Korea, under Grant 22A20130000045, in part by the International Collaborative Research and Development Program funded by the Ministry of Trade, Industry and Energy, South Korea, in part by the National Research Foundation of Korea funded by the South Korean Government (MEST) under Grant 2011-0017495, and in part by the Industrial Strategy Technology Development Program of the Ministry of Trade, Industry and Energy under Grant 10039673. The Associate Editor for this paper was J. A. Barria. *(Corresponding author: Myoungho Sunwoo.)*

The authors are with the Automotive Control and Electronics Laboratory, Department of Automotive Engineering, Hanyang University, Seoul 04763, South Korea (e-mail: msunwoo@hanyang.ac.kr).

Color versions of one or more of the figures in this paper are available online at http://ieeexplore.ieee.org.

Digital Object Identifier 10.1109/TITS.2018.2855183

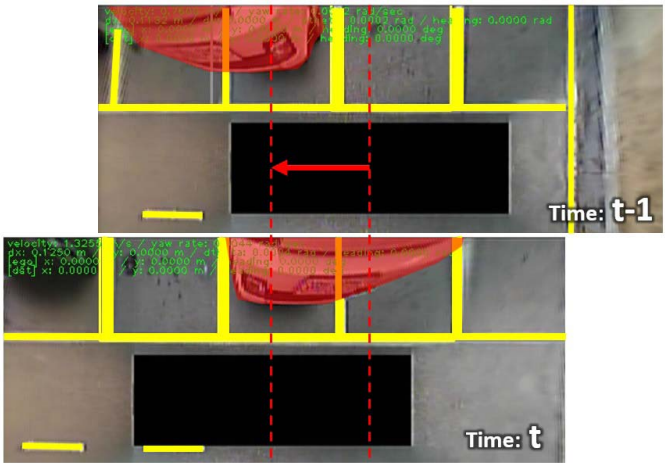

Fig. 1. Distortion of a 3D object in successive AVM images. (Yellow lines: road surface marker, Red arrows: direction of movement in images, Red area: 3D object, Black area: ego vehicle).

When a 3D object such as a parked vehicle is recognized by an AVM system, the shape of the vehicle is distorted and occupies an empty space in a parking area, as shown in Fig. 1. When a false-positive feature of the parking slot marker is detected from the parked vehicle, it is recognized as a no-parking space or an occupied space, even though it is an empty parking space. Moreover, since a distorted 3D object occludes the parking slot marker, the parking slot marker cannot be detected even when it exists. An AVM system also cannot detect the parking slot marker under the ego vehicle on which the AVM camera is attached. Thus, the feature directly extracted from the AVM image can cause mis-recognition of the parking space and failure of the autonomous parking system.

In previous studies, the random finite set statistics method, the probabilistic hough transform and many other methods were used to reduce false-positive features in feature extraction [7]–[12]. However, these methods were highly affected by 3-D objects and could not provide accuracy for the extracted feature. The methods reduced the false-positive features from the shadow of objects such as trees and surrounding vehicles. Unlike the shadow of objects, the shadow of the ego vehicle is the same position of the AVM images. The shadow of the ego vehicle does not follow the motion of the camera. Since the introduced methods do not consider the motion of the camera, they are not suitable for filtering the false-positive features caused by the shadow of the ego vehicle.

In this paper, we propose an occupancy probability filter to overcome the limitation of previous studies. The proposed filter applies a Bayesian filtering scheme for the image coordinate to estimate the probability using a series of AVM images. Each pixel of the AVM image has an occupancy probability of containing a parking slot marker. The occupancy probabilities from previous

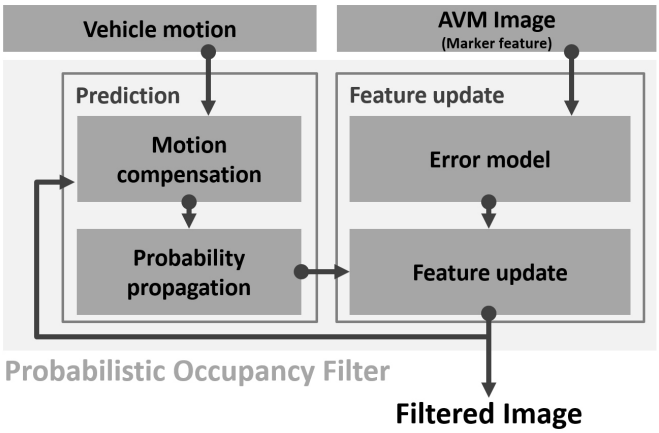

Fig. 2. Algorithm structure of the probabilistic occupancy filter.

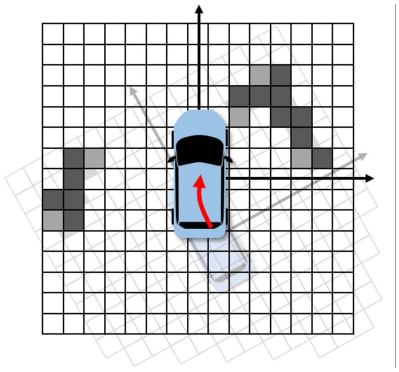

Fig. 3. Motion compensation for a temporal AVM image (Gray cells: compensated occupancy probability, Red arrow: vehicle motion).

locations compensate for the vehicle motion information, and the occupancy probabilities are propagated as shown in the prediction step of Fig. 2. The predicted occupancy probability is updated using the error model of the AVM and performance index of the feature extractor when the AVM image is updated as the feature update step of Fig. 2.

II. Prediction

A. Motion Compensation

Since the AVM provides a series of images over time, the AVM image changes when the ego vehicle position changes. Therefore, to predict the current occupancy probability from the previous occupancy probability, the previous occupancy probability compensates for the change in position of the ego vehicle, as shown in Fig. 3. By compensating for this change in the previous image, the occupancy probability of the road surface marker in the previous AVM image can be reflected into the current AVM image. The position of the occupancy probability is updated by rotation matrix R_t and translation matrix using the measured motion information.

The rotation motion of the AVM image is generated from the ego vehicle yaw motion, which is measured by a yaw-rate sensor. Since the previous AVM image is rotated in the opposite direction of the measured yaw-rate, the amount of the rotation angle is calculated by multiplying the yaw-rate $-\dot{\varphi}_t$ and the period Δt of the updated AVM image. Therefore, the rotation matrix R_t is estimated using a linear conversion rule as described in (1).

$$R_t = \begin{bmatrix} cos(-\dot{\varphi}_t \Delta t) & -sin(-\dot{\varphi}_t \Delta t) \\ sin(-\dot{\varphi}_t \Delta t) & cos(-\dot{\varphi}_t \Delta t) \end{bmatrix} \quad (1)$$

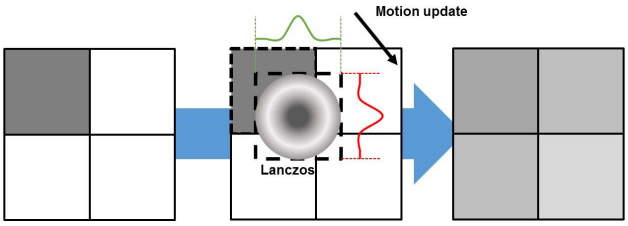

Fig. 4. Lanczos interpolation method for each occupancy probability.

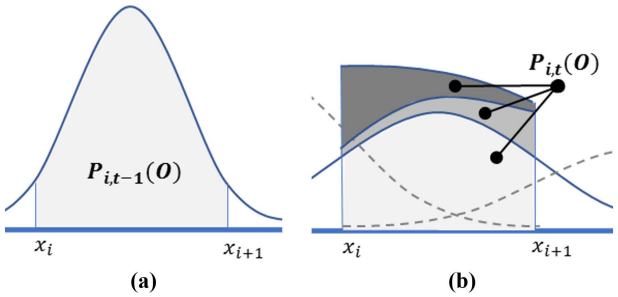

Fig. 5. Propagated occupancy probability by the surrounding probabilities: (a) Prior probability, (b) Propagated probability.

The translation of the AVM image is generated by the ego vehicle motion in the heading direction. The direction of the AVM image translation is the opposite direction of the ego vehicle motion, which can be measured by a wheel speed sensor. Thus, the current position of the occupancy probability X_t is predicted from the previous position X_{t-1} using the estimated rotation matrix and translation as described in (2).

$$[x_t, y_t]^T = R_t \cdot [x_{t-1}, y_{t-1}]^T + \begin{bmatrix} -v_t \Delta t \\ 0 \end{bmatrix} \quad (2)$$

The moved position of the previous pixel does not exactly match the pixel of the current image. The occupancy probabilities for the pixels of the current image are approximated using the Lanczos method, which is an interpolation method based on a normalized $sinc$ function, as shown in Fig. 4 [13].

B. Probability Propagation

The compensation of the vehicle motion of the previous image has an uncertainty because of noise from the sensor and the inaccuracy of the compensation model. When the occupancy probability of each pixel follows a Gaussian distribution, the occupancy probability in the pixel is shown in Fig. 5-(a). The Gaussian distribution is predicted by the belief propagation of a Bayesian filter using the noise model $p(t|t-1, u_t)$ as described in (3). This Gaussian distribution is propagated as a Bayesian filter if the noise of the compensation model has white Gaussian noise.

$$p_{i,j,t}(x_t, y_t) = \int p(t|t-1) p_{i,j,t-1}(x_{t-1}, y_{t-1}) dx dy \quad (3)$$

The propagated distribution at pixel (x,y) is represented as $p_{i,j,t}(x, y)$. When the co-variance of the propagated distribution at pixel (x,y) increases, the occupancy likelihood of the parking slot marker in the surrounding pixels increases. Since the occupancy probability $P_{i,j,t}(O)$ of this pixel is also affected by the distribution of the surrounding pixels, the occupancy probability of pixel can be predicted by summing the area under the surrounding distribution as shown in Fig. 5-(b). The occupancy probability of the current AVM image $P_{i,j,t}(O)$ is predicted as described in (4). This probability

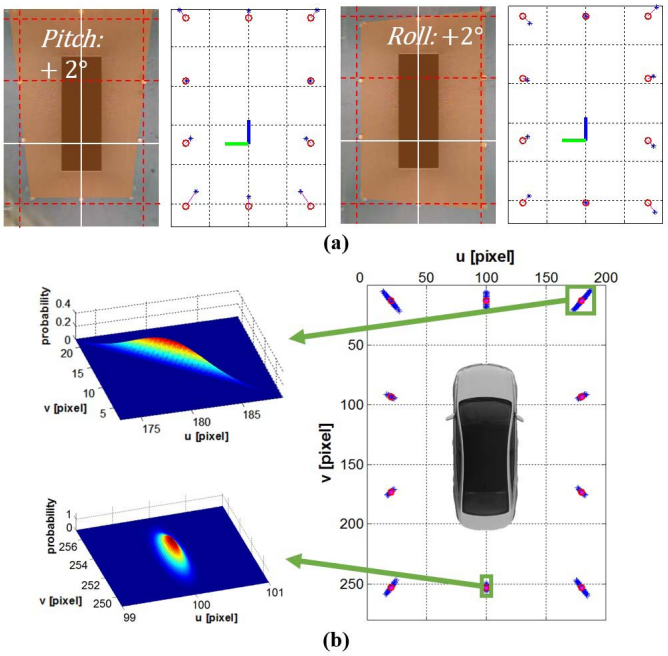

Fig. 6. Error model for the AVM image: (a) Effects of the motion of the ego vehicle, and (b) Error distribution of each pixel.

summation of the surrounding pixels is estimated by operating on a Gaussian kernel, which is generated from the co-variance of the compensation model.

$$p_{i,j,t}(O) = \sum \int_{y_j}^{y_{j+1}} \int_{x_i}^{x_{i+1}} p_{i,j,t}(x_t, y_t) dx dy \tag{4}$$

III. Feature Update

A. Measurement Error Model Generation

A measurement error for a parking slot marker of the AVM image appears when there is a roll or pitch motion of the ego vehicle. The error model for the measurement error should be obtained in advance before extracting the parking slot marker from the AVM image. If there is a parking slot marker near the ego vehicle, the AVM image is predicted by the geometry relationship between the camera pose and the parking slot marker. The geometry relationship is affected by the motion of the ego vehicle such as the roll or pitch motion as shown in Fig. 6-(a). The error distribution of the parking slot marker is obtained using the geometry relationship between the camera and the parking slot marker and the roll or pitch motion of the ego vehicle. The Gaussian distribution is used to model the error distribution of each pixel in the AVM image as shown in Fig. 6-(b) [14], [15]. To obtain the discrete probability distribution for each pixel, the Gaussian kernel is generated using the Gaussian error distribution. The Gaussian kernel of each pixel $P_{i,j,meas}$ is used to calculate the occupancy probability of each pixel in the current AVM image, as described in (5) and (6).

A feature extractor is used to extract a parking slot marker feature from the AVM image. False Positives (FPs), which are incorrect positive extractions, and False Negatives (FNs), which are incorrect negative extractions, occur when the parking slot marker feature is extracted from the AVM image using the feature extractor as shown in Fig. 7. The performance of the feature extractor for the parking slot marker is evaluated by comparing the AVM image and the result of the feature extractor for the parking slot marker. The True-Positive rate R_{TP} and False-Positive rate R_{FP} are obtained by evaluating the

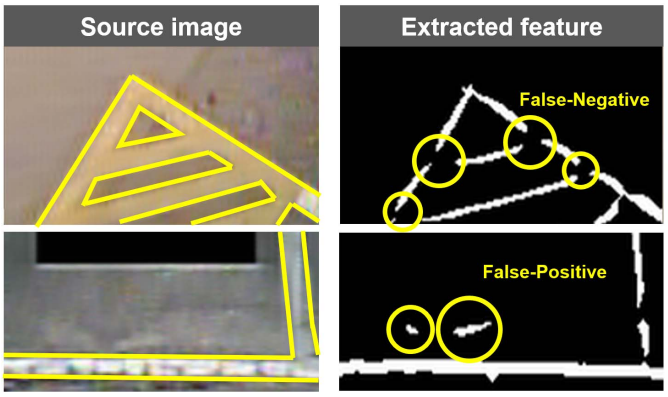

Fig. 7. False negative and false positive in the extracted parking slot marker feature.

performance of the AVM feature extractor. The TP rate R_{TP} is the ratio of the number of True-Positive (TP) pixels to the sum of the number of TP and FN pixels when the parking slot marker feature exists. The FP rate R_{FP} is the ratio of the number of FP pixels to the sum of the number of FP and True-Negative (TN) pixels when there is no parking slot marker feature.

The Gaussian kernel, which is generated using the Gaussian error distribution, and the evaluation result of the parking slot marker extractor are used to calculate the occupancy probability in the current AVM image. $P_{i,j,t}(Z|O)$ is the probability that each pixel of the current AVM image is occupied when there is a parking slot marker. $P_{i,j,t}(Z|O)$ is obtained by using the TP rate R_{TP} and the Gaussian kernel of each pixel of the AVM image as described in (5).

$$P_{i,j,t}(Z|O) = R_{TP} \cdot P_{i,j,meas} \tag{5}$$

$P_{i,j,t}(Z|\bar{O})$ is the probability that each pixel of the current AVM image is occupied when there is no parking slot marker. $P_{i,j,t}(Z|\bar{O})$ is obtained by using the FP rate FP rate R_{FP} and the Gaussian kernel of each pixel of the AVM image as described in (6).

$$P_{i,j,t}(Z|\bar{O}) = R_{FP} \cdot P_{i,j,meas} \tag{6}$$

B. Occupancy Probability Update

The AVM image provides a top-view image using multiple cameras equipped on the vehicle. The cameras do not detect several areas that are occluded by the ego vehicle or outside the field of view of the AVMS. Therefore, the AVM image consists of two parts: a detectable area and an undetectable area. The detectable area is predicted by the motion compensation and probability propagation of the previous AVM image. The current occupancy probability of each pixel in the current image is updated using the predicted probability from the previous AVM image and the occupancy probability of the parking slot marker extractor. However, in the undetectable area, the occupancy probability of the parking slot marker in the current AVM image cannot be used to update the current occupancy probability because of the undetectable area outside the field of view of the AVM. Thus, the undetectable area is updated using only the predicted probability from the previous AVM image.

The Bayes rule is used to update the current occupancy probability of the detectable area. $P_{i,j,t}(Z)$ is the probability that the current AVM image is occupied by the feature. The probability $P_{i,j,t}(Z)$ is defined in (7).

$$P_{i,j,t}(Z) = P_{i,j,t}(Z|O)P_{i,j,t}(O) + P_{i,j,t}(Z|\bar{O})P_{i,j,t}(\bar{O}) \tag{7}$$

TABLE I
SPECIFICATIONS OF THE SENSORS

Sensor	Update rate [ms]	Resolution	Noise (RMS)
Yaw-rate sensor	10	0.0625	0.5 deg/s
Wheel speed sensor	10	0.035	0.3 m/s
AVM	50	320x240	-

$P_{i,j,t}(O|Z)$ is the occupancy probability that there is a parking slot marker feature at each pixel when the current AVM image is occupied by the feature. The probability $P_{i,j,t}(O|Z)$ can be obtained as shown in (8) [16]. $P_{i,j,t}(O)$ is the probability that each pixel of the predicted AVM image is occupied by the feature. The updated occupancy probability is used to determine whether each pixel in the AVM image is occupied.

$$P_{i,j,t}(O|Z) = \frac{\sum_{i,j}^{k} P_{i,j,t}(Z|O) P_{i,j,t}(O)}{\sum_{i,j}^{k} P_{i,j,t}(Z)} \tag{8}$$

IV. EXPERIMENTS

The experiments were conducted using a test vehicle equipped with vehicle motion sensors such as wheel speed sensors, and a yaw-rate sensor. Since the yaw rate can be filtered with a simple mathematical model, a yaw-rate sensor is used for estimating the rotation motion in the experiment. The sensor measurements were obtained from the Controller Area Network (CAN) without installing additional sensors. The specifications of the sensors that are used for the evaluation of the proposed algorithm are described in Table I. Each pixel of the image provided from the AVM image represents 0.0328 meters.

In the experiments, a pillbox kernel is used for the slot marker extraction from the AVM image [17]. To evaluate the effectiveness of the proposed filter, the results of the probabilistic occupancy filter and extracted features are compared with the ground truth, which was manually labeled in three cases: parking slot marker occlusion by the ego vehicle, false-positive feature from the shadow, and false-positive feature from 3D objects. The proposed filter was verified in 16,455 frames obtained from the three different parking conditions such as asphalt (outdoor) and urethane (outdoor and indoor). The proposed method was evaluated with the metric of the false-positive rate, and the metric of previous studies to compare the performance.

A. Scenario I: Occluded Features

AVM provides an image where the center area is empty because the markers are occluded by the ego vehicle. For example, the end line is occluded when there is perpendicular parking, as shown in Fig. 8-(d). The guidance marker is occluded while the vehicle is moving in the parking lot, as shown in Fig. 8-(a). In this case, there is no parking slot marker in the ego vehicle location of the original image, so the slot marker feature cannot be extracted, as shown in Fig. 8-(b), (e).

Occluded markers are important features for direct vehicle localization to calculate the relative positions for vehicle control in parking assistance systems and autonomous parking systems. Self-localization can fail because of these occluded features, and necessary information to control the vehicle such as the parking end line cannot be obtained.

The AVM provides an identical image to the top view at the current vehicle position. Thus, the markers on the road surface move as much as the vehicle movement. Even if the occupancy probability is propagated by the uncertainty of the vehicle motion, the occupancy probability increases when the AVM image of the next step is updated. When the serial AVM images are accumulated to obtain the occupancy probability of the parking slot marker, where the marker features are occluded by the ego vehicle can be reconstructed, as shown in Fig. 8-(c), (f). Based on the reconstructed information, the parking slot can be recognized from the filtered feature without an additional compensation algorithm. Moreover, these filtered features can be used for vehicle control.

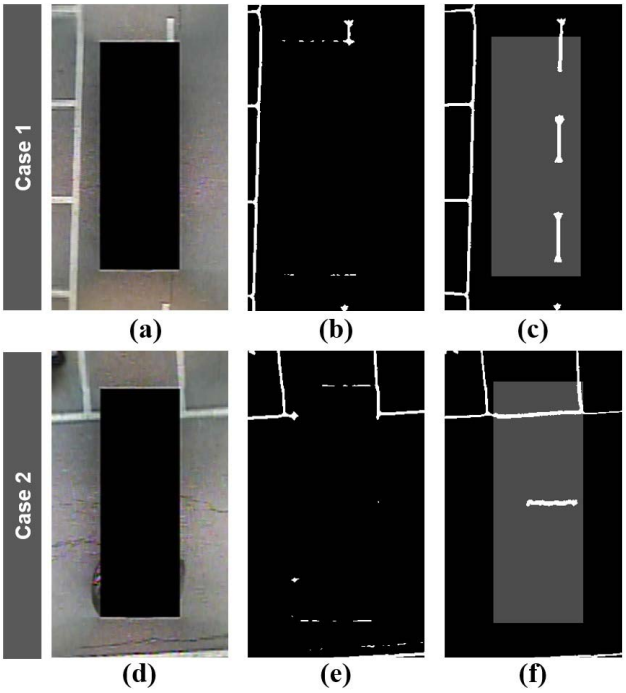

Fig. 8. Reconstructing the occluded road surface marker: (a), (d) Source image, (b), (e) Extracted feature, (c), (f) Result of the proposed filter.

B. Scenario II: Shadows

Since the AVM image shows the surroundings of the vehicle, there is a vehicle shadow. A large portion of the image is affected by shadows as shown in the red circles in Fig. 9-(a), (d). The false-positive feature is extracted in a shadow, as shown in the red circles in Fig. 9-(b), (e). The detected false-positive feature causes false parking space recognition because the feature is extracted from the nearby ego vehicle.

The shadows in the AVM are generated by ambient light sources such as fluorescent lights or sunlight. Thus, the motion of a shadow in the AVM image does not follow the vehicle motion. Even if the occupancy probability is updated at the shadow once in a moving scene, the occupancy probability is not repeated at the predicted position by the vehicle motion in the next scene. Therefore, the occupancy probability of the shadow decreases. As a result, the occupancy probability of the slot marker extracted from the shadow decreases. When the serial AVM images are accumulated to obtain the occupancy probability of the parking slot marker, the shadow is not recognized as a parking marker, as shown in the red circles in Fig. 9-(c), (f). As verified in this case, the number of false-positives from shadows can be reduced by applying the proposed filter. Specifically, the false-positive rate is reduced from 0.51% to 0.05% by applying the proposed probabilistic occupancy filter.

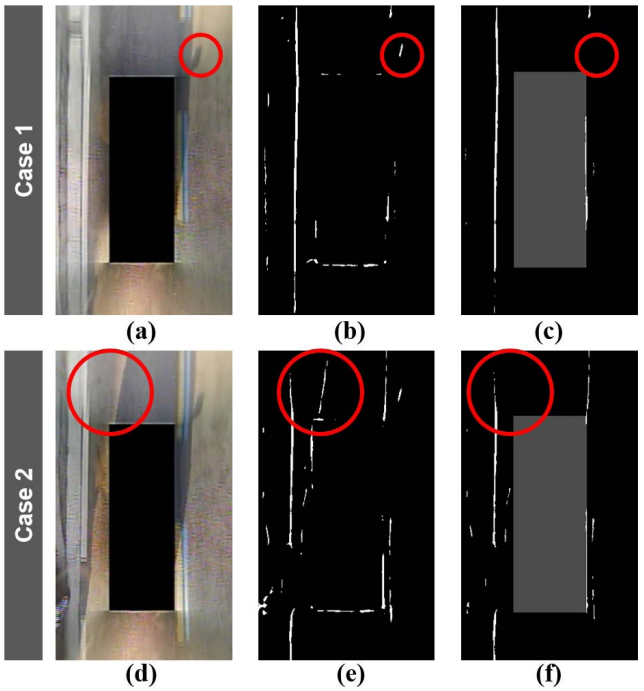

Fig. 9. Reducing false-positives from the shadow (a), (d) Source image, (b), (e) Extracted feature, and (c), (f) Result of the proposed filter.

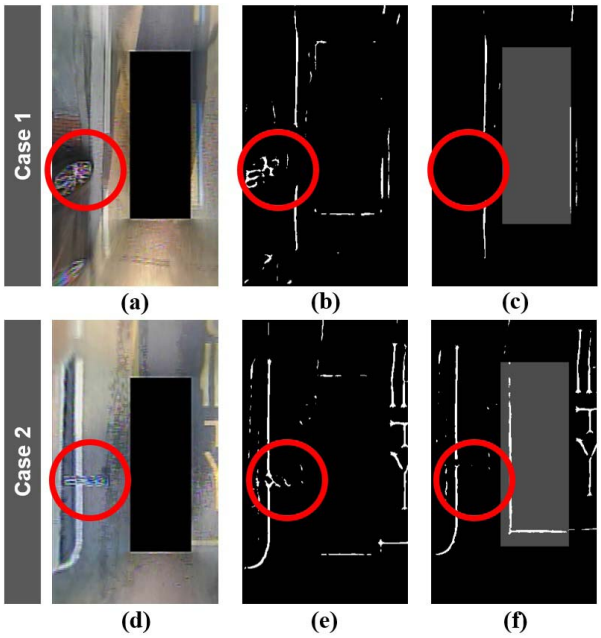

Fig. 10. Reducing false-positives from 3D objects (a), (d) Source image, (b), (e) Extracted feature, and (c), (f) Result of the proposed filter.

C. Scenario III: 3D Objects

Since an AVMS provides a top-view like image by merging multiple camera images instead of the actual top-view images, the 3D objects are distorted in the AVM image because of the merging process. The parked vehicle seems to occupy a side empty space, as shown in the red circles of Fig. 10-(a). The guidance cone is deformed, as shown in the red circles in Fig. 10-(d). If a false positive occurs from distorted 3D objects, as shown in the red circles in Fig. 10-(b), (e), the 3D objects can be mis-recognized as a parking slot marker. This false-positive also distorts the shape of the parking slot marker.

The shapes of 3D objects in the AVM image varies depending on the position where they are measured. Thus, the motion of 3D objects in the AVM image does not follow the vehicle motion. Even if the occupancy probability is updated at 3D objects when they are in a moving scene, the occupancy probability is not repeated at the predicted position by the vehicle motion in the next scene. Therefore, the occupancy probability of the slot marker extracted from 3D objects decreases. When the serial AVM images are accumulated to obtain the occupancy probability of a parking slot marker, the 3D objects are not recognized as a parking marker, as shown in the red circles in Fig. 10-(c), (f). It is possible to reduce the false positives from 3D objects by applying the proposed filter. The false-positive rate is reduced from 0.63% to 0.04% by applying the proposed probabilistic occupancy filter.

D. Comparison With Previous Methods

To check the feasibility of the proposed algorithm, we compared the result using the evaluation metrics proposed in the previous studies. The results are compared in the data set achieved by the test vehicle. When the proposed filter is evaluated using the accuracy as a comparison metric, the proposed filter was better than the Canny edge method, local threshold, and anisotropy steerable filter, as shown in Table II. The proposed filter has about a 4.75% improvement in accuracy, as compared with the accuracy of the anisotropy steerable filter [8]. Moreover, when the false rate is used for the comparison metric, the proposed method reduced the false rate by about 1.95%, as compared with the PHD filter, as shown in Table III [9].

TABLE II
COMPARISON RESULTS ABOUT ACCURACY

Filters	Accuracy (%)
Anisotropy steerable filter [7]	92.82
Randomized hough transform [12]	95.2
Local threshold [7]	95.54
Canny edge method [8]	96.58
Probabilistic hough transform [10]	96.9
Proposed filter	**97.57**

TABLE III
COMPARISON RESULTS ABOUT FALSE RATE

Filter	false rate (%)
Anisotropic steerable filter [11]	6.42
PHD filter [9]	6.2
Proposed filter	**4.25**

V. CONCLUSION

AVM sensor-based parking slot marker detection has an occlusion problem and a false-positive problem from other objects such as shadows and 3D objects. In this paper, we propose a probabilistic filter to overcome these problems.

The proposed probabilistic occupancy filter uses two inputs: a series of AVM images and the measured vehicle motion from on-board sensors. In this filter, each pixel of an AVM image is represented as the occupancy probabilities of a parking slot marker by using the AVM error model.

As evaluated in the experiments, the proposed filter reduces the occlusion effect and false-positive rate from other objects. Thus, this

filter has several advantages to overcome the problems of AVM-based parking slot marker detection.

- It reconstructs the feature occluded by an ego vehicle using a series of AVM images.
- It reduces the false-positive features from shadows and 3D objects, using the characteristics of AVM images.

The proposed filter is suitable for where a scene is repeated with different conditions, such as parking. However, because the filter uses vehicle motion information, it is difficult to remove false positive features if the extracted false positive features follow the motion of a vehicle (e.g., a shadow of another object) or the vehicle is stationary. This framework can be applied to detect parking slot markers or all types of road surface markers, such as lane and road signs.

The occupancy probability of the proposed filter can be applied as the weight of the feature matching. We plan to apply this probability to improve the performance of feature-matching-based vehicle localization systems.

REFERENCES

[1] W.-J. Park, B.-S. Kim, D.-E. Seo, D.-S. Kim, and K.-H. Lee, "Parking space detection using ultrasonic sensor in parking assistance system," in *Proc. IEEE IVS*, Jun. 2008, pp. 1039–1044.

[2] V. Agarwal, N. V. Murali, and C. Chandramouli, "A cost-effective ultrasonic sensor-based driver-assistance system for congested traffic conditions," *IEEE Trans. Intell. Transp. Syst.*, vol. 10, no. 3, pp. 486–498, Sep. 2009.

[3] A. Kianpisheh, N. Mustaffa, P. Limtrairut, and P. Keikhosrokiani, "Smart parking system (SPS) architecture using ultrasonic detector," *Int. J. Softw. Eng. Appl.*, vol. 6, no. 3, pp. 55–58, 2012.

[4] J. K. Suhr and H. G. Jung, "Sensor fusion-based vacant parking slot detection and tracking," *IEEE Trans. Intell. Transp. Syst.*, vol. 15, no. 1, pp. 21–36, Feb. 2014.

[5] H. G. Jung, D. S. Kim, P. J. Yoon, and J. Kim, "Parking slot markings recognition for automatic parking assist system," in *Proc. IEEE Intell. Vehicles Symp.* Jun. 2006, pp. 106–113.

[6] C. Wang, H. Zhang, M. Yang, X. Wang, L. Ye, and C. Guo, "Automatic parking based on a bird's eye view vision system," *Adv. Mech. Eng.*, vol. 6, p. 847406, Mar. 2014.

[7] T. Veit, J.-P. Tarel, P. Nicolle, and P. Charbonnier, "Evaluation of road marking feature extraction," in *Proc. IEEE ITSC*, Oct. 2008, pp. 174–181.

[8] C. Li, N. Qi, X. Yang, and B. Dai, "Road markings feature extraction from omni-directional image," in *Proc. Chin. Automat. Congr. (CAC)*, Oct. 2017, pp. 1223–1228.

[9] F. Zhang, H. Stähle, C. Chen, C. Buckl, and A. Knoll, "A lane marking extraction approach based on random finite set statistics," in *Proc. 4th IEEE Intell. Vehicles Symp.*, Jun. 2013, pp. 1143–1148.

[10] G. Bacchiani, M. Patander, A. Cionini, and D. Giaquinto, "Parking slots detection on the equivalence sphere with a progressive probabilistic Hough transform," in *Proc. IEEE 20th Int. Conf. Intell. Transp. Syst. (ITSC)*, Oct. 2017, pp. 1–6.

[11] C. Li, B. Dai, R. Wang, Y. Fang, X. Yuan, and T. Wu, "Multi-lane detection based on omnidirectional camera using anisotropic steerable filters," *IET Intell. Transp. Syst.*, vol. 10, no. 5, pp. 298–307, 2016.

[12] P. Mongkonyong, C. Nuthong, S. Siddhichai, and M. Yamakita, "Lane detection using randomized Hough transform," in *Proc. IOP Conf. Ser., Mater. Sci. Eng.* London, U.K.: IOP, vol. 297, no. 1. 2018, p. 012050.

[13] W. Burger and M. J. Burge, *Principles of Digital Image Processing*. London, U.K.: Springer, 2009.

[14] K. Jo, Y. Jo, J. K. Suhr, H. G. Jung, and M. Sunwoo, "Precise localization of an autonomous car based on probabilistic noise models of road surface marker features using multiple cameras," *IEEE Trans. Intell. Transp. Syst.*, vol. 16, no. 6, pp. 3377–3392, Dec. 2015.

[15] S. Thrun, "Probabilistic robotics," *Commun. ACM*, vol. 45, no. 3, pp. 52–57, 2002.

[16] D. Simon, *Optimal State Estimation: Kalman, H Infinity, and Nonlinear Approaches*. Hoboken, NJ, USA: Wiley, 2006.

[17] S.-J. Han and J. Choi, "Parking space recognition for autonomous valet parking using height and salient-line probability maps," *ETRI J.*, vol. 37, no. 6, pp. 1220–1230, 2015.